JOURNAL OF COMPUTATIONAL PHYSICS **120,** 305–315 (1995)

Spline-Galerkin Solution of Dynamic Equations for Particle Comminution and Collection

D. EYRE

*Institute of Advanced Scientific Computation, The University of Liverpool, Liverpool, United Kingdom and Department of Mathematics and Applied Mathematics Potchefstroom University for CHE, Potchefstroom, Republic of South Africa**

Received June 3, 1994; revised February 21, 1995

The population balance equation is solved for particles undergoing a combination of growth, comminution, and collection. The approximation method is to use a weighted Galerkin technique with cubic B-splines and an implicit scheme for solving the system of ordinary differential equations. The cubic splines are defined on a graded mesh. The performance of the method is investigated by solving a model problem with simple but nonsmooth kernels. The weight function is chosen so that singularities in the equation can be easily treated. A self-similar solution for comminuted particles is shown to be a useful representation for the solution of the population balance equation provided that this equation is solved over a sufficiently long time interval. Stationary solutions of the equation are obtained for a model that describes both particle comminution and collection.

1. INTRODUCTION

Consider a dispersed phase system where random collisions between particles lead to their subsequent breakup into smaller particles and/or coalescence to form larger particles. In the parlance of population balance the process of collision and subsequent breakup of particles is referred to as *comminution,* while the process of collision and subsequent coalescence of particles is referred to as *collection.*

It is clear that comminution and collection are competing processes that have opposite effects on the distribution of particle sizes, comminution leads to an increase in the number of particles but a decrease in the average particle size, while collection leads to a decrease in the number of particles but an increase in the average particle size. Both effects may occur in a number of physical systems, for example, gas bubbles in a liquid (Barigou and Graves [2]) and liquid–liquid dispersions (Tobin *et al.* [18]). For these systems a stationary (time-independent) distribution of particle sizes can result. The particle size distribution may provide useful insight into the effects of turbulence that are responsible for particle breakup.

The random collision is a stochastic process. The stochastic equations that describe particle comminution and collection can be solved using Monte Carlo simulation techniques (see, for example, Prince and Blanch [14]). An alternative approach is to solve a deterministic equation, usually referred to as the *population balance equation.* This equation describes the changes in the average particle size distribution and can approximately reproduce the true stochastic averages. A review of the status of population balances and numerical techniques for the solution of the equations is given by Ramkrishna [15]. A successful numerical approach has been to use a finite element method where the basis functions are chosen to be splines [9].

The aim of the present paper is to develop a numerical method to solve the population balance equation for comminution, together with collection and growth, where the kernels as well as the solution function can be either singular or nonsmooth. By nonsmooth it is meant that derivatives of the function are singular, for example, $\sqrt{x}$ is a nonsmooth function with an infinite derivative at $x = 0$.

The numerical approach is to perform a spatial discretisation of the equations using a projection technique on a space of cubic splines. The flexibility of smoothest splines means that these functions can be used to describe structure in the solution function. The usual approach has been to determine the spline coefficients from a collocation method [8, 9]. Attempts have been made using these methods to investigate the effects of turbulence in the framework of the population balance equation [16]. More recently, however, Erasmus *et al.* [7] make use of cubic *B*-splines and a Galerkin technique to treat a nonsmooth behaviour in the growth term of the Lifshitz–Slyozov equation of continuity. The method is used to solve the population balance equation for a combination of collection and growth (a change in particle size that is not due to an interaction between the particles themselves).

In the present paper the spline–Galerkin technique is used to solve the population balance equation for comminuted particles. An important consideration for comminuting particles is that the growth of small particles due to the breakup of larger particles may result in the emergence of a singularity in the particle size distribution for particles of zero size. (This does not mean, however, that there are an infinite number of zero sized particles.)

* Present address.

0021-9991/95 $12.00

The Galerkin technique reduces the problem of solving the partial integro-differential equation to that of solving a system of ordinary differential equations and evaluating moment integrals of the kernel functions. An important difference between the present method and other methods that are usually based on some type of collocation approach is that while the collocation method requires the evaluation of one-dimensional moment integrals the moment integrals that arise in the Galerkin approach are two dimensional. Since the basis functions are cubic polynomials the additional integral can be used more effectively to smooth singular (on nonsmooth) behaviour in the kernels. The technique is used to solve a simple model problem of particle breakup as well as problems involving coalescence and growth.

The population balance equation is described in Section 2, where a simple model is chosen for growth, comminution and collection. Section 3 describes the discretization of the equations, where special attention is given to treating singularities that can arise. Numerical examples that test the performance of the method, as well as some numerical results are presented in Section 4. The conclusions are given in Section 5.

2. DYNAMICAL MODEL

Let $n(v, t)\,dv$ be the number density, that is the number of particles per unit volume with volumes that lie in the interval between v and $v + dv$ at time t. The number density function, $n(v, t)$, satisfies the equation

$$\frac{\partial}{\partial t} n(v, t) + \frac{\partial}{\partial v} [I(v) n(v, t)] = \mathcal{B}(v, n(v, t)) + \mathcal{C}(v, n(v, t)). \tag{2.1}$$

The second term on the left-hand side is a growth term that describes the change in the number density function due to a change in the particle size. Here $I(v) = \dot{v}$ is the growth rate of a particle of volume v. Terms $\mathcal{B}$ and $\mathcal{C}$ describe the change in the number of particles due to comminution and collection, respectively. It will be assumed that there is a sufficiently low density of particles that only two-body collisions dominate the comminution and collection processes.

The comminution term is

$$\mathcal{B}(v, n(v, t)) = -s(v) n(v, t) + \int_v^\infty s(v') b(v, v') n(v', t)\, dv'. \tag{2.2}$$

Here $b(v, v')\,dv$ is a dimensionless quantity that describes the fraction of particles with volumes between v and $v + dv$ that result from the breakup of larger particles. We refer to $b(v, v')$ as the *breakup function*. The function $s(v)$ is a *selection function*, with units of inverse time, that describes the rate at which particles of volume v are broken into smaller fragments. The interpretation of the terms on the right-hand side of Eq. (2.2) can be understood as follows: the first term represents the loss of particles of volume v due to breakup into smaller particles, while the second term represents the increase of particles of volume v resulting from the breakup of particles larger than v.

The collection term is

$$\mathcal{C}(v, n(v, t)) = \frac{1}{2} \int_0^v n(v', t) n(v - v', t) k(v', v - v')\, dv' - n(v, t) \int_0^\infty n(v', t) k(v', v)\, dv', \tag{2.3}$$

where $k(v', v)$ is the *collection kernel* for two particles of volume v' and v and has units of volume/time. The collection kernel describes both the geometry and dynamics of the collection mechanism. The first term on the right-hand side of Eq. (2.3) represents the increase of particles of volume v due to coalescence of two smaller particles. The factor of $\frac{1}{2}$ prevents overcounting. The second term represents the loss of particles of volume v as a result of their coalescing with particles of any volume.

The solution of Eq. (2.1) is subject to both initial and boundary conditions. The initial condition is

$$n(v, 0) = w_0(v), \tag{2.4}$$

where $w_0(v)$ is the initial number density function. The boundary condition is required only for the case of a nonzero growth term, I. A physically reasonable boundary condition is

$$n(0, t) = 0, \tag{2.5}$$

which assumes that there are no particles of zero size.

It is important to recognize that the functions b and k satisfy certain constraints. The breakup function, b, satisfies the integral identity

$$\int_0^v \frac{v'}{v} b(v', v)\, dv = 1. \tag{2.6}$$

The breakup function is often written

$$b(v, v') = \frac{v'}{v} \frac{\partial}{\partial v} \Psi\left(\frac{v}{v'}\right), \tag{2.7}$$

where Ψ is a univariate function. The constraint on the breakup function given by Eq. (2.6) means that Ψ satisfies the equation

$$\int_0^1 \frac{d}{dx} \Psi(x)\, dx = 1. \tag{2.8}$$

This constraint on b (and Ψ) ensures that the probability that a particle of volume v will break up into smaller fragments

with volumes that sum to v is unity. The constraint placed on the collection kernel, k, is that it is a symmetric function of its arguments.

$$k(v, v') = k(v', v), \tag{2.9}$$

indicating that the formation of a particle of volume $(v + v')$ from the coalescence of two smaller particles with volumes v and v' is unique.

A useful representation of the particle distribution is obtained by taking moments of the number density function. The ith moment is defined by

$$M_i(t) = \int_0^\infty n_i(v, t)\, dv, \quad n_i(v, t) = n(v, t)v^i. \tag{2.10}$$

(Where no confusion should arise the zero subscript of $n_0(v, t)$ will be dropped.) The zeroth moment, $M_0(t)$, corresponds to the total number density of particles. The total initial number density, $M_0(0)$, will be denoted by N_0. The first moment, $M_1(t)$, corresponds to the total volume density. For zero growth, $I = 0$, the constraints given by Eqs. (2.6) and (2.9) lead to the conservation of total volume density, namely

$$\frac{d}{dt} M_1(t) = 0. \tag{2.11}$$

Analytic solutions of the population balance equation have been obtained for a number of special cases. Usually such a solution can be found only for simple choices of the functions I, k, s, and Ψ. In the present work it will be assumed that these functions have the form

$$I(v) = F_\gamma v^\gamma, \tag{2.12}$$

$$k(v, v') = \frac{H_\rho}{2}(v^\rho + v'^\rho). \tag{2.13}$$

$$s(v) = G_\alpha v^\alpha, \tag{2.14}$$

and

$$\Psi\left(\frac{v}{v'}\right) = \left(\frac{v}{v'}\right)^\beta. \tag{2.15}$$

The functions given above are typical in much of the work on analytic solutions of the population balance equation [9, 12, 17]. Also the selection and breakup functions given above have been used, within the context of a discrete comminution model, to describe comminution of mineral bearing ores in mill grinding (see, for example, Austin *et al.* [1]). The combination of comminution and collection for these situations has also been suggested [10].

Similarity solutions for comminuted particles using the above selection and breakup functions have been reported by Kapur [11] and for a wider class of breakup functions by Peterson [13]. Since the similarity solution provides a useful insight into the comminution equation a brief description of the similarity solution obtained by Kapur [11] will now be given. We begin by writing the comminution equation

$$\frac{\partial}{\partial t} n(v, t) = \mathcal{B}(v, n(v, t)) \tag{2.16}$$

in its more usual form

$$\frac{\partial}{\partial t} n_1(v, t) = -s(v)n_1(v, t) + \int_v^\infty s(v') \frac{\partial}{\partial v} \Psi\left(\frac{v}{v'}\right) n_1(v', t)\, dv'. \tag{2.17}$$

Note that, for a constant density ρ, the volume v and mass $m = \rho v$ are interchangable as independent variables. When the mass variable is used in Eq. (2.17) it is usually referred to as the *mass balance equation.*

The basic idea behind the similarity approach is to obtain solutions that are the same when expressed in terms of a certain transformed variable. In other words, the solutions are self-similar to one another. In the case of Eq. (2.17) it is possible to obtain such a similarity solution by introducing the dimensionless group

$$n_2(v, t) = pZ(p), \quad p = \frac{v}{M_2(t)}. \tag{2.18}$$

From $s(v) = G_\alpha v^\alpha$ and Eq. (2.17), it follows that M_2 satisfies

$$\frac{d}{dt} M_2(t) = -G_\alpha c M_2(t)^\alpha, \tag{2.19}$$

where c is a constant. Equation (2.19) has the solution

$$M_2(t) = \left(\frac{1}{M_2(0)^\alpha} + G_\alpha c\alpha t\right)^{-1/\alpha}. \tag{2.20}$$

The function $Z(p)$ satisfies

$$cp \frac{d}{dp} Z(p) = -(p^\alpha + c)Z(p) + \int_p^\infty p'^\alpha \frac{\partial}{\partial p} \Psi\left(\frac{p}{p'}\right) Z(p')\, dp'. \tag{2.21}$$

In the special case $\Psi(v/v') = (v/v')^\beta$ this equation has the solution

$$Z(p) = C_0 p^{\beta-1} \exp\left(-\frac{p^\alpha}{\alpha c}\right), \tag{2.22}$$

where

$$C_0 = \frac{\alpha M_1}{(\alpha c)^{\beta/\alpha}\Gamma(\beta/\alpha)}, \tag{2.23}$$

$$c = \frac{1}{\alpha M_1}\left[\frac{\Gamma(\beta/\alpha)}{\Gamma((\beta+1)/\alpha)}\right]^\alpha, \tag{2.24}$$

and Γ is the gamma function.

3. APPROXIMATION METHOD

We begin this section by writing the population balance equation in a dimensionless form that is suitable for the spline approximation. Let ζ be a characteristic volume that represents some average particle volume. Since the actual particle volumes can vary over several orders of magnitude it is convenient to introduce a dimensionless volume on a finite interval $x \in [-1, 1]$ via a nonlinear mapping

$$\frac{v}{\zeta} = \frac{1+x}{1-x}. \tag{3.1}$$

A dimensionless variable of the time is $\tau = N_0\chi t$, where χ is a characteristic rate constant. The dependent variable $n(v, t)$ is now transformed to a function of dimensionless arguments,

$$\tilde{n}(x, \tau) = \frac{\zeta}{N_0}\frac{2}{(1-x)^2} n(v, t). \tag{3.2}$$

The initial function $w_0(v) = n(v, 0)$ is similarly transformed so that

$$\tilde{w}_0(x) = \frac{\zeta}{N_0}\frac{2}{(1-x)^2} w_0(v). \tag{3.3}$$

The transformed function $\tilde{n}(x, \tau)$ satisfies the dimensionless population balance equation

$$\frac{\partial}{\partial\tau}\tilde{n}(x, \tau) + \lambda_a \frac{\partial}{\partial x}[\alpha(x)\tilde{n}(x, \tau)] = \lambda_b \tilde{b}(x, \tilde{n}(x, \tau)) + \lambda_c \tilde{c}(x, \tilde{n}(x, \tau)), \tag{3.4}$$

where

$$\tilde{b}(x, \tilde{n}(x, \tau)) = -\sigma(x)\tilde{n}(x, \tau) + \int_x^1 \sigma(x')\delta(x, x')\tilde{n}(x', \tau)\, dx', \tag{3.5}$$

$$\tilde{c}(x, \tilde{n}(x, \tau)) = \frac{1}{2}\int_{-1}^{x} \tilde{n}(x', \tau)\tilde{n}(u, \tau)\kappa(x', u)\left(\frac{1-u}{1-x}\right)^2 dx' - \tilde{n}(x, \tau)\int_{-1}^{1} \tilde{n}(x', \tau)\kappa(x', x)\, dx', \tag{3.6}$$

$u = u(x', x)$ is the transformed volume difference

$$u = \frac{2(x-x') - (1-x)(1-x')}{2(x-x') + (1-x)(1-x')} \tag{3.7}$$

and

$$\alpha(x) = (1+x)^\gamma(1-x)^{(2-\gamma)}; \tag{3.8}$$

$$\sigma(x) = \left(\frac{1+x}{1-x}\right)^\alpha, \tag{3.9}$$

$$\delta(x, x') = \frac{2\beta}{(1+x)^{(2-\beta)}(1-x)^\beta}\left(\frac{1+x'}{1-x'}\right)^{(1-\beta)}, \tag{3.10}$$

$$\kappa(x', x) = \left(\left(\frac{1+x}{1-x}\right)^\rho + \left(\frac{1+x'}{1-x'}\right)^\rho\right). \tag{3.11}$$

The dimensionless rate constants are

$$\lambda_a = \frac{\zeta^{\gamma-1}}{2N_0\chi}F_\gamma, \quad \lambda_b = \frac{\zeta^\alpha}{N_0\chi}G_\alpha, \quad \lambda_c = \frac{\zeta^\rho}{\chi}H_\rho. \tag{3.12}$$

The constants λ_a, λ_b, and λ_c can be used to determine the relative importance of dynamic processes in the population balance equation. For example, a dimensionless measure of the comminution/collection rates is given by the ratio

$$\Lambda_{b,c} = \frac{\lambda_b}{\lambda_c}. \tag{3.13}$$

For $\Lambda_{b,c} \gg 1$ comminution dominants the collection process, while for $\Lambda_{b,c} \ll 1$ collection will dominate comminution. For $\Lambda_{b,c} = 1$ the particle size spectrum is subject to approximately equal rates of comminution and collection.

Discretisation of the dimensionless population balance equation is carried out on a space of cubic splines. The assumption here is that $\tilde{n}(x, \tau)$ falls off sufficiently rapidly that

$$(1-x)^{-\nu}\tilde{n}(x, \tau) \to 0 \quad \text{as } x \to 1 \text{ for } \nu > 0. \tag{3.14}$$

Thus there are no singularities at the right-hand side of the interval at $x = 1$. Care is taken, however, to ensure that spurious singularities do not arise in the discretization of the equations, that is, when $\tilde{n}(x, \tau)$ is approximated by a spline. For this purpose a cutoff parameter, x_c, is introduced so that the interval over which the problem is defined now becomes $[-1, x_c]$. The actual choice of cutoff parameter will depend on the problem

to be solved, the mapping parameter ζ, and the total time interval over which the solution is being sought.

Cubic B-splines on $x \in [-1, x_c]$ are constructed as follows: The interval is partitioned by m nodal points $\{x_i\}_{i=1}^m$, where $-1 = x_1 < x_2 < \cdots < x_m = x_c$. Additional points are placed at the ends of this interval, namely, $x_{-2} \leq x_{-1} \leq x_0 \leq x_1$ and $x_m \leq x_{m+1} \leq x_{m+2} \leq x_{m+3}$. Define

$$B_i^{(1)}(x) = \begin{cases} (x_i - x_{i-1})^{-1}, & x_{i-1} < x \leq x_i, \\ 0, & \text{otherwise.} \end{cases} \tag{3.15}$$

The B-splines of order l (degree $l - 1$) are generated by the stable iterative method of Cox [4] and deBoor [5],

$$B_i^{(l)}(x) = \frac{(x - x_{i-l})B_{i-1}^{(l-1)}(x) - (x_i - x)B_i^{(l-1)}(x)}{x_i - x_{i-l}}. \tag{3.16}$$

Note that the index on the cubic B-splines runs from $i = 2, ..., m + 3$. A convenient notation is $B_i(x) = B_{i+2}^{(4)}(x)$ to denote the cubic B-spline which is nonzero over the interval (x_{i-2}, x_{i+2}) so that the index now runs from $i = 0, ..., m + 1$.

The (unknown) solution is approximated by the linear combination

$$\tilde{n}_A(x, \tau) = \sum_{j=0}^{m+1} f_j(\tau)B_j(x). \tag{3.17}$$

Substituting this approximation for the solution in the population balance equation leads to a residual function

$$\begin{aligned} r(x, \tau) = \frac{\partial}{\partial \tau}\tilde{n}_A(x, \tau) + \lambda_a \frac{\partial}{\partial x}[\alpha(x)\tilde{n}_A(x, \tau)] \\ - \lambda_b \tilde{b}(x, \tilde{n}_A(x, \tau)) - \lambda_c \tilde{c}(x, \tilde{n}_A(x, \tau)). \end{aligned} \tag{3.18}$$

For the case $\lambda_a = 0$ the coefficients $\{f_i\}_{i=0}^{m+1}$ are obtained from a weighted Galerkin method by solving the $(m + 2)$ equations

$$\int_{-1}^{x_c} B_j(x)r(x, \tau)\omega(x)\,dx = 0, \quad k = 0, ..., (m + 1), \tag{3.19}$$

where $\omega(x)$ is the weight factor. For the case where $\lambda_a \neq 0$ the boundary condition is incorporated by replacing the first equation (for $k = 0$) by a discrete form of the boundary condition. This modification will be described after performing the temporal discretization of the equations.

The problem now reduces to that of solving the system of ordinary differential equations

$$L\dot{\mathbf{f}}(\tau) = -(\lambda_a A + \lambda_b B)\mathbf{f}(\tau) + \lambda_c \mathbf{f}^{\mathrm{T}}(\tau)C\mathbf{f}(\tau), \tag{3.20}$$

for the expansion coefficients $\mathbf{f} = (f_0, f_1, ..., f_{m+1})^{\mathrm{T}}$. The matrices L, A, B, and C are given by

$$L_{i,j} = \int_{-1}^{x_c} B_i(x)B_j(x)\omega(x)\,dx, \tag{3.21}$$

$$\begin{aligned} A_{i,j} = &\int_{-1}^{x_c} B_i(x)B_j'(x)\alpha(x)\omega(x)\,dx \\ &+ \int_{-1}^{x_c} B_i(x)B_j(x)\alpha'(x)\omega(x)\,dx, \end{aligned} \tag{3.22}$$

$$\begin{aligned} B_{i,j} = &\int_{-1}^{x_c} B_i(x)B_j(x)\sigma(x)\omega(x)\,dx \\ &- \int_{-1}^{x_c} B_i(x)\omega(x)\left(\int_x^{x_c} B_j(x')\sigma(x')\delta(x, x')\,dx'\right)dx, \end{aligned} \tag{3.23}$$

and

$$\begin{aligned} C_{i,j,k} = &\frac{1}{2}\int_{-1}^{x_c} B_i(x)\omega(x) \\ &\left(\int_{-1}^{x} B_j(u)B_k(x')\kappa(x', u)\left(\frac{1-u}{1-x}\right)^2 dx'\right)dx \\ &- \int_{-1}^{x_c} B_i(x)B_j(x)\omega(x)\left(\int_{-1}^{x_c} B_k(x')\kappa(x', x)\,dx'\right)dx. \end{aligned} \tag{3.24}$$

The moment integrals A and B may contain singular integrands. For the case $0 < \gamma < 1$ the growth term in Eq. (2.12) is a nonsmooth function with an infinite derivative at $x = -1$. A method for treating this type of nonsmooth behaviour has been dealt with in the work of Erasmus *et al.* [7] and can easily be incorporated into the present method for solving the comminution/collection equation. Singularities arising from the growth term will therefore not be discussed further in this paper. Singularities that arise in the communation term, however, require further consideration and a more detailed investigation of these singularities will now be given.

Following from Eq. (3.10) the dimensionless breakup function factorizes in the variables x and x' and the comminution coefficient becomes

$$\begin{aligned} B_{i,j} = &-\int_{-1}^{x_c}\left(\frac{1+x}{1-x}\right)^{\alpha} B_i(x)B_j(x)\omega(x)\,dx \\ &+ 2\beta\int_{-1}^{x_c}\frac{B_i(x)\omega(x)}{(1+x)^{(2-\beta)}(1-x)^{\beta}} \\ &\left(\int_x^{x_c}\left(\frac{1+x'}{1-x'}\right)^{(1+\alpha-\beta)} B_j(x')\,dx'\right)dx. \end{aligned} \tag{3.25}$$

Difficulties can arise in the second term of Eq. (3.25) for particular choices of the exponents α and β. The second term may contain a number of singularities. For example, if $\beta < 2$

the outer integral contains a singularity at $x = -1$. Also the inner integral contains a singular term if $\beta > (1 + \alpha)$. To ensure that this second singularity does not occur the value of β will be restricted by the constraint

$$\beta \leq 1 + \alpha. \tag{3.26}$$

This means that the condition necessary for a singularity at $x = -1$ is satisfied for $\alpha < 1$. The unwanted singularity in the outer integral is removed by choosing a weight factor $\omega(x) = (1 + x)^{2-\beta}$.

The exponent ρ determines the shape of the coalescence function and therefore the underlying collection mechanism. There is no restriction on ρ, which in principle can take any value including a negative value. Special cases for the collection kernel, which will be used in the present study, include the constant kernel, $\rho = 0$, and the Golovin kernel, $\rho = 1$. These special cases may be considered as two limiting cases of a diffusion process for coalescence. Values of ρ that lie outside this range will therefore not be considered.

Discretizing the initial condition (2.4) leads to an expression for the initial spline coefficients $\{f_i(0)\}_{i=0}^{m+1}$,

$$\sum_{j=0}^{m+1} B_j(x) f_j(0) = \tilde{w}_0(x), \tag{3.27}$$

One way to obtain these coefficients is to collocate and solve the algebraic system

$$\sum_{j=0}^{m+1} B_j(u_i) f_j(0) = \tilde{w}_0(u_i). \tag{3.28}$$

The collocation approach is useful if the initial condition is given only on a set of data points, $\tilde{w}_0(u_i)$, rather than as the function $\tilde{w}_0(x)$. Note, however, that to obtain a solvable system requires at least the same number of collocation points $\{u_i\}$ as there are coefficients $\{f_i(0)\}$. (Additional collocation points can be used in which case a least squares approximation is employed to determine the coefficients.) There is some freedom in the choice of the collocation points, although in practice the placement of these points is restricted by the Schoenberg–Whitney theorem (de Boor [6, p. 200, Theorem XIII.1]) which requires that $u_i \in (x_{i-2}, x_{i+2})$. The choice adopted in the present paper is to place one collocation point at each nodal point. The two additional points, needed to obtain a solvable system, are placed at the midpoint of each end interval. Thus

$$\begin{aligned} &u_0 = x_1; && u_1 = \tfrac{1}{2}(x_1 + x_2); \\ &u_i = x_i, && i = 2, \ldots, m-1; \\ &u_m = \tfrac{1}{2}(x_m + x_{m+1}); && u_{m+1} = x_m, \end{aligned} \tag{3.29}$$

Next we turn to the question of temporal discretization. We introduce the time step $\Delta\tau$. Time is now expressed in terms of an index $r = \tau/\Delta\tau$, while the coefficient $f_{j,r}$ denotes an approximation to $f_j(\tau)$.

A classical one-step θ-method gives

$$\begin{aligned} L\mathbf{f}_{r+1} - \theta\Delta\tau((\lambda_a A + \lambda_b B)\mathbf{f}_{r+1} - \lambda_c \mathbf{f}_{r+1}^T C \mathbf{f}_{r+1}) \\ = L\mathbf{f}_r + (1-\theta)\Delta\tau((\lambda_a A + \lambda_b B)\mathbf{f}_r - \lambda_c \mathbf{f}_r^T C \mathbf{f}_r). \end{aligned} \tag{3.30}$$

Here the value of θ can be varied from $\theta = 0$ (explicit scheme) to $\theta = 1$ (fully implicit scheme). The value of $\theta = \frac{1}{2}$ gives the Crank–Nicolson method. The set $\mathbf{f}_r$ is used as an initial estimate. An implicit scheme is recommended [3] for solving the comminution/collection equation.

The required boundary condition for the case $\lambda_a \neq 0$ has the discrete approximation

$$\sum_{j=0}^{3} B_i(-1) f_{j,r+1} = 0. \tag{3.31}$$

This replaces the first equation (for $k = 0$) in the algebraic system (3.19).

The source code is written in Fortran 90 and makes full use of features such as modules, array syntax, and dynamic storage allocation. Unfortunately, at present Fortran 90 does not support a standard library and a number of routines had to be constructed for the purpose of solving the discrete equations. Gauss elimination is used to solve the algebraic equations, while the nonlinear equations are solved using an iterative method. Integrals are evaluated numerically using a standard Gauss–Legendre quadrature formula.

4. NUMERICAL EXAMPLES

An initial condition is required for the numerical examples. The family of initial conditions used by Scott [17] is

$$w_0(v) = \frac{N_0}{v_0} \frac{(\xi+1)^{(\xi+1)}}{\Gamma(\xi+1)} \left(\frac{v}{v_0}\right)^{\xi} \exp\left(-\frac{v}{v_0}(\xi+1)\right), \tag{4.1}$$

where $\xi \geq 0$. The moments are $M_0(0) = N_0$ and $M_1(0) = v_0 N_0$. Thus v_0 is the initial average particle volume. Although the case $\xi = 0$ does not satisfy the boundary condition in Eq. (2.5) it can be used for solutions that do not include the growth term. The parameters $N_0 = 1$ and $v_0 = 2$ are used for all numerical calculations.

A number of simple test problems are now considered. These test problems are referred to as Examples 1 through 7. The parameter $\chi = 1$ is used in all calculations so that time is measured as a dimensionless quantity. In addition to the initial condition parameter, ξ, and the volume scale parameter, ζ, the model has up to four shape parameters α, β, ρ, and γ as well as the three rate constants G_α, H_ρ, and F_γ. For convenience

TABLE I

Tabulation of Numerical Examples

Example	ξ	ζ	α	β	ρ	γ	G_α	H_ρ	F_γ
1	1	1	0.8	1.2	—	—	1	—	—
2	0	1	0.8	1.2	0	—	1	1	—
3	1	1	0.8	1.2	0	—	1	1	—
4	1	1	0.8	1.2	0	—	2	1	—
5	1	1	0.8	1.2	1	—	1	1	—
6	1	10	0.8	1.2	0	1	0.1585	1	1

Note. Example 1 is the "pure" comminution equation with an initial condition given by Eq. (4.1) with $\xi = 1$. Example 2 is a comminution plus collection equation with a constant collection kernel and initial condition $\xi = 0$. Example 3 is the same as Example 2 but with initial condition $\xi = 1$. In Example 4 the comminution term is a factor two larger than in Example 3. Example 5 is a comminution plus collection equation with a Golovin collection kernel. Example 6 is an equation that combines comminution, collection (with a constant kernel), and growth.

these parameters have been tabulated in Table I. A cuttoff parameter $x_c = 0.96$ is used for all test problems. An implicit scheme ($\theta = 1$) is used to solve the system (3.30) with time step $\Delta\tau = 0.01$.

Our first results concern the comminution equation (2.16) of Example 1. This example is used to test the performance of the numerical method for treating the problem of particle comminution.

The choice of nodal points is expected to play an important role in determining the accuracy of the numerical approximation. Nodal points in the cubic spline approximation must be placed in the interval $[-1, x_c]$. For this purpose a set of $(m-2)$ points, $\{q_i\} \in [-1, 1]$, are mapped to the nodal points $\{x_i\} \in [-1, x_c]$ using the transformation

$$x_i = (x_c + 1)(q_i + 1)/2 - 1, \quad i = 2, ..., m-1. \tag{4.2}$$

Let $h = 2/(m-1)$. A uniform distribution of points is given by

$$q_i = (i-1)h - 1, \quad i = 2, ..., m-1. \tag{4.3}$$

Figure 1 shows the computed solution, $\tilde{n}_1(x, \tau)$, using $m = 38$ nodes on a uniformly spaced mesh. Curves are shown at dimensionless time intervals of 0.5. It is clear that the computed solution is oscillating at the left-hand side of the interval. The oscillation becomes worse as time increases. The oscillatory behaviour is caused by a steep slope in the solution function on the left-hand end of the interval (near $x = -1$). Indeed, the similarity solution (Eq. (2.22)) has the asymptotic behaviour $Z(p) \to p^{0.2}$ as $p \to 0$. One way to improve the accuracy of the numerical solution on a mesh of given size is to concentrate the nodal points in a region where the solution function has a rapidly varying structure. In the present case this can be achieved, for example, by choosing the graded mesh

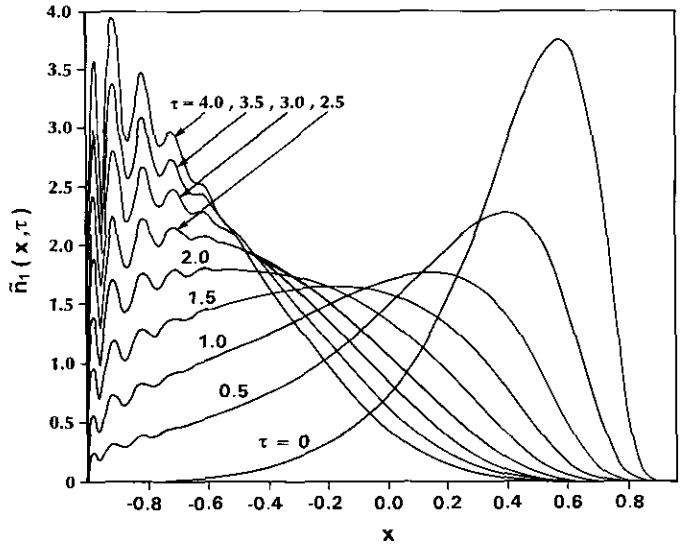

FIG. 1. Solution of the comminution equation (Example 1) using $m = 38$ nodal points on a uniform mesh. Curves show the result for $\tilde{n}_1(x, \tau)$ at time intervals of 0.5 up to $\tau = 4$.

$$q_i = -\cos\left((i-1)h\frac{\pi}{2}\right), \quad i = 2, ..., m-1. \tag{4.4}$$

Other choices of mesh are also possible (for example, an equidistribution of points based on arc length and curvatures [8]). Figure 2 shows the computed solution using the graded mesh (4.4). Since the graded mesh provides a more accurate solution of the comminution problem than the mesh based on uniformly distributed nodes it is therefore used for all subsequent calculations.

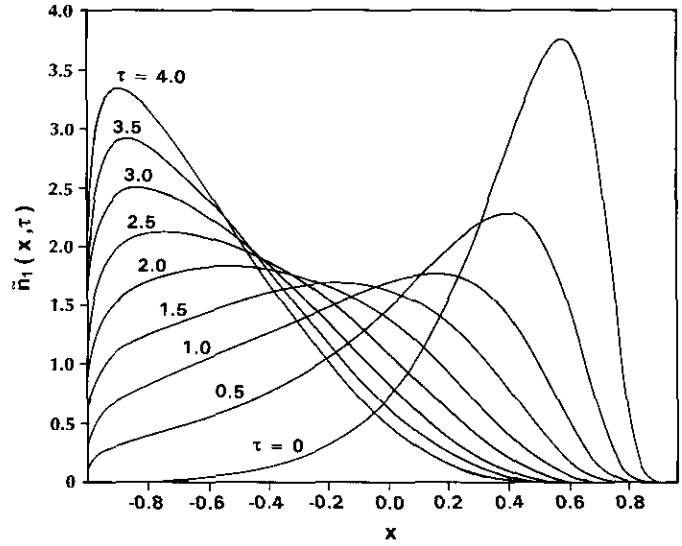

FIG. 2. Same as Fig. 1 but using the graded mesh in Eq. (4.4).

TABLE II

Computed Moments $M_0(\tau)$, $M_1(\tau)$, and $M_2(\tau)$ for the Comminution Equation of Example 1

τ	$M_0(\tau)$	$M_1(\tau)$	$M_2(\tau)$
0.0	1.00	2.000	6.000
0.5	4.88	2.006	3.408
1.0	9.17	2.010	2.234
1.5	13.77	2.012	1.605
2.0	18.60	2.015	1.227
2.5	23.62	2.017	0.979
3.0	28.80	2.018	0.808
3.5	34.12	2.019	0.682
4.0	39.55	2.021	0.588

The computed moments, $M_0(\tau)$, $M_1(\tau)$, and $M_2(\tau)$, for example 1 are tabulated in Table II. Here $m = 98$ nodes have been used. The total number of particles, $M_0(\tau)$, increases with increasing time, while the moment $M_2(\tau)$ decreases with increasing time. The total volume, on the other hand, is a conserved quantity with the value $M_1 = 2$. The small deviation of the computed solution from this value (about 1% at $\tau = 4$) is due to the numerical approximation. In order to check convergence of the numerical method Table III shows the results at $\tau = 4$ for different values of m. Also shown are the work units as measured by the CPU time. The work unit is an indication of the computational effort required to solve the equation. It can be seen that the computational effort increases approximately quadratically with increasing mesh size. Equation (2.20) gives a value of $M_2(4) = 0.613$. This, however, is predicted by the similarity method and can therefore only be considered an approximation to the exact value of the moment $M_2(4)$. The computed moments of $M_2(4)$ show approximately linear convergence towards a value slightly smaller than that predicted by the similarity method.

Conservation of volume can be built into the numerical method by renormalizing the approximate solution after a number of time steps. Table IV shows the computed moments $M_0(4)$ and $M_2(4)$ obtained by normalizing the approximate solution after each time step, $\Delta\tau = 0.01$. (The results shown in Table IV did not change significantly when the solution was normalized after longer time intervals of $\tau = 0.5$.) The results for $M_2(4)$ show a marked improvement for smaller values of m, while the results for $M_0(4)$ show no significant improvement when compared with the unnormalized results. The reason for this is that $M_2(4)$ emphasises the large particle size behaviour of the particle size distribution which is better reproduced by the normalization procedure. On the other hand, $M_0(4)$ is sensitive to the solution function at the small particle end of the particle size spectrum. In the region the normalization procedure does not improve the spline approximation of the singular solution function.

TABLE III

Computed Solution of the Comminution Model (Example 1) at $\tau = 4$ Using $m + 2$ Cubic B-splines

$m + 2$	$M_0(4)$	$M_1(4)$	$M_2(4)$	Work units
20	37.68	2.123	0.626	50
30	38.85	2.077	0.608	102
40	39.34	2.055	0.601	190
60	39.61	2.036	0.593	455
80	39.60	2.026	0.590	942
100	39.55	2.021	0.588	1632

Note. The exact moment $M_1(4) = 2.0$ while Eq. (2.20) of the similarity method predicts a value $M_2(4) = 0.613$. Work units are measured by the CPU time (in seconds).

TABLE IV

Computed Solution of the Comminution Model (Example 1) at $\tau = 4$ Using $m + 2$ Cubic B-Splines

$m + 2$	$M_0(4)$	$M_2(4)$
20	35.49	0.589
30	37.42	0.586
40	38.28	0.584
60	38.92	0.583
80	39.09	0.582
100	39.15	0.582

Note. The solution has been normalized so that $M_1 = 2.0$ at each time step.

It should be remarked that the degree to which the unnormalized solution satisfies the conservation rule is a measure of how well the method is able to obtain a solution of the population balance equation. Given the above discussion it is clear that this provides a useful check on the computed solution in cases where the exact solution is singular.

Figure 3 shows the solution to Example 1 as a function of the variable $p = v/M_2(t)$ plotted on a log scale. Curves are shown for the computed solution $Z(p)$ at dimensionless time intervals of 0.5. These curves correspond to the same solution as those of Fig. 2. The similarity solution of Eq. (2.22) is also shown by a broken line. Comparing the long time behaviour of the numerical solution with the similarity solution it can be seen that, at least for large values of p, the curves in Fig. 3 converge towards the similarity solution which it approaches after a time $\tau \gg 1$. However, in the region of small p it is not clear that the similarity solution is reproduced by the numerical results. The reason for this is that the spline function is being used to approximate a singular function at $p = 0$. Nevertheless, the computed solution does continue to increase towards the similarity solution as τ increases. Comparing the results shown in Fig. 2 with those in Fig. 3 it can be seen that the similarity solution emerges only after the initial function (labeled as $\tau = 0$ in Fig. 2) is mostly "washed out" by the effects of particle comminution.

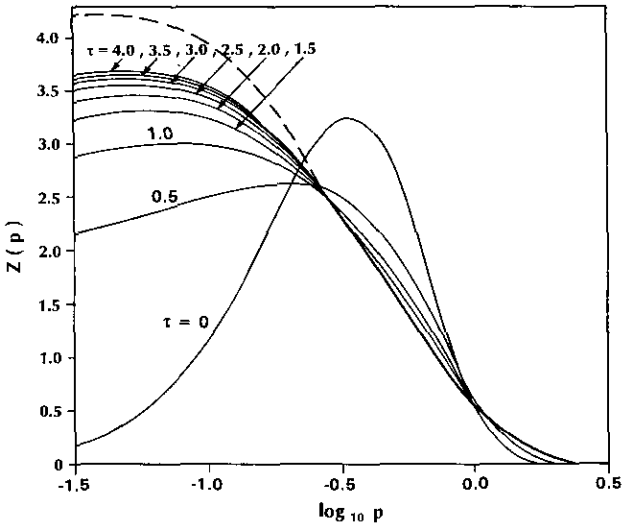

FIG. 3. Solution of the comminution equation (Example 1). Curves show the result for $Z(p)$ at time intervals of 0.5. Broken line is the similarity solution of Equation (2.22).

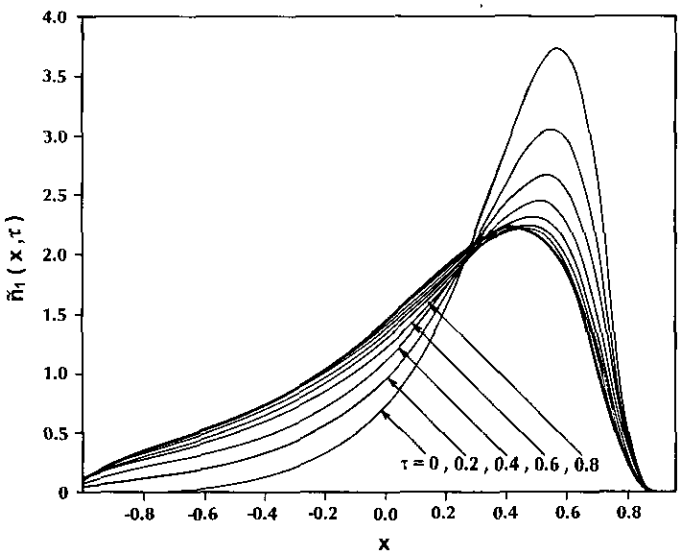

FIG. 5. Solution of the comminution/collection equation with initial parameter $\xi = 1$ (Example 3, Example 2).

Next we turn to the comminution/collection equation. Figures 4 to 7 show the computed solutions for Examples 2 to 5, respectively. The first results are for a constant collection kernel and a dimensionless comminution/collection rate of $\Lambda_{b,c} = 1$. Figure 4 shows $\tilde{n}_1(x, \tau)$ for an initial condition $\xi = 0$ (Example 2). The computed solution is shown at dimensionless time intervals of 0.2. After about $\tau = 2$ the computed solution does not change. This stationary solution results from a balance between the effects of particle comminution and collection. Figure 5 shows the computed solution starting from a different initial condition $\xi = 1$ (Example 3). Again the same stationary solution is obtained which would suggest that this stationary solution is an attractor. The computed moments, $M_0(\tau)$ and $M_1(\tau)$, for Example 3 are tabulated in Table V. The total number of particles is seen to converge towards a value of $M_0 \approx 4$. Results at $\tau = 2$ for different values of m are shown in Table VI. Convergence of the moments is similar to that found in the case of "pure" comminution. For this nonlinear problem, however, the work units increase approximately with the cube of the mesh size. By changing the dimensionless comminution/collection ratio, a different stationary solution is obtained. Figure 6 shows the computed solution for $\Lambda_{b,c} = 2$ (Example 4). Clearly increasing the rate of comminution has produced a stationary solution that has a larger number of small particles and a smaller number of large particles. In other words the distribution of particle sizes has moved to the left. Figure 7

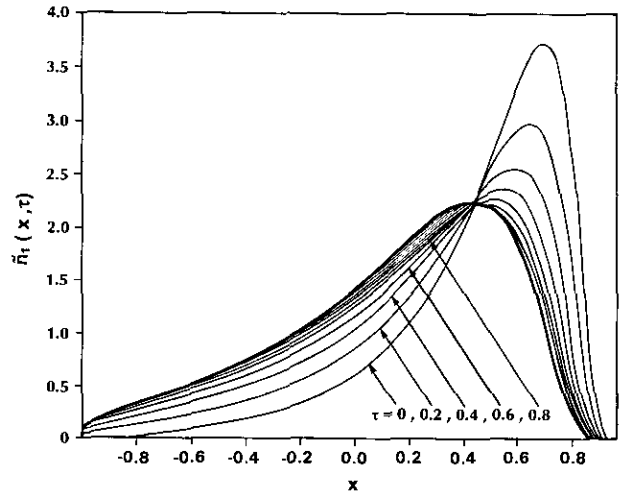

FIG. 4. Solution of the comminution/collection equation with initial parameter $\xi = 0$ (Example 2). Curves show the result for $\tilde{n}_1(x, \tau)$ at time intervals of 0.2.

TABLE V

Computed Moments $M_0(\tau)$ and $M_1(\tau)$ for the Comminution/Collection Equation of Example 3

τ	$M_0(\tau)$	$M_1(\tau)$
0.0	1.00	2.000
0.2	2.26	2.003
0.4	3.11	2.006
0.6	3.61	2.008
0.8	3.88	2.011
1.0	4.02	2.013
1.2	4.09	2.015
1.4	4.12	2.017
1.6	4.14	2.019
1.8	4.16	2.021
2.0	4.16	2.023

TABLE VI

Computed Solution of the Comminution/Coalescence Model (Example 3) at $\tau = 2$ Using $m + 2$ Cubic B-Splines

$m + 2$	$M_0(2)$	$M_1(2)$	Work units
20	4.04	2.139	116
30	4.08	2.036	319
40	4.10	2.062	688
60	4.14	2.040	2182
80	4.15	2.029	5107
100	4.16	2.023	10061

Note. The exact moment $M_1(2) = 2.0$. Work units are measured by the CPU time (in seconds).

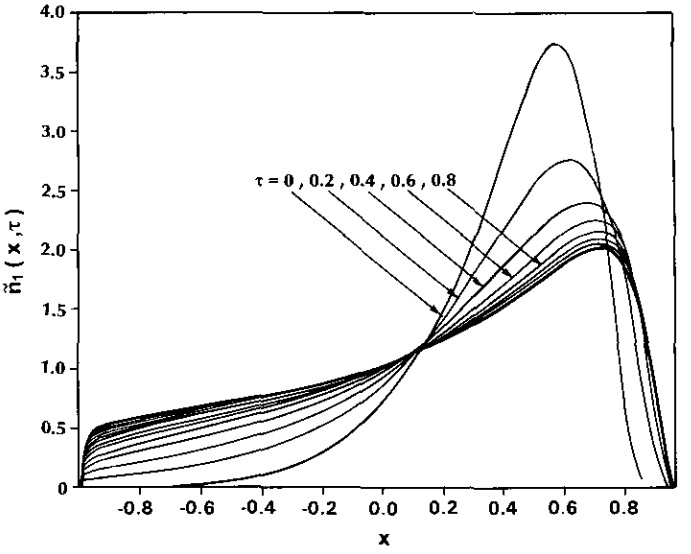

FIG. 7. Solution of the comminution/collection equation for a Golovin collection kernel (Example 5).

shows the result for the Golovin collection kernel (Example 5). Here the distribution of particle sizes is spread out to produce a stationary solution with a more flattened distribution profile.

Our final results concern the inclusion of particle growth. Again the dimensionless comminution/collection rate is chosen to be $\Lambda_{b,c} = 1$ (Example 6). Figure 8 shows the computed solution for this problem. Note that due to the effects of particle growth the area enclosed by the curves for $\tilde{n}_1(x, \tau)$ increases with increasing τ. This is in marked contrast to the previous examples, where M_1 was a conserved quantity for the population balance equation. Due to the presence of a growth term the particle size distribution does not reach a stationary solution.

5. CONCLUSIONS

A spline–Galerkin method has been described for the accurate numerical solution of the population balance equation for growth, comminution, and collection of particles. To obtain accurate solutions for comminuted particles it was found necessary to introduce a graded mesh. The similarity solution can provide a useful representation for the solution of the population balance equation for comminuted particles, but only on the large particle end of the particle size spectrum and only for large times, $\tau \gg 1$. For short times, $\tau \approx 1$, and particularly for small particles, the similarity solution may not be accurate because the initial function can still influence the comminution process.

An important result for particles undergoing a combination of

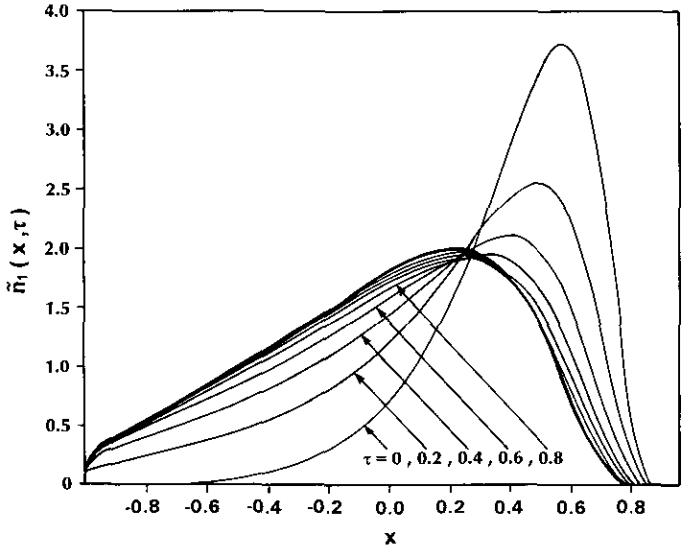

FIG. 6. Solution of the comminution/collection equation with comminution term a factor of two larger than in Example 3 (Example 4).

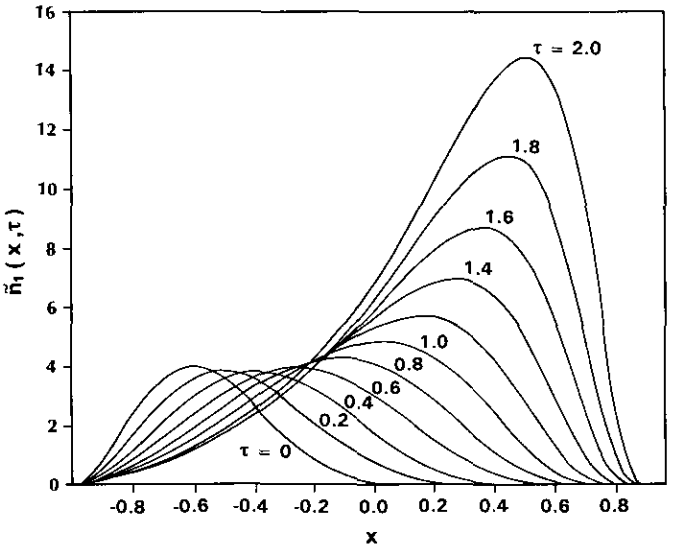

FIG. 8. Solution of the comminution/collection equation with growth (Example 6). Curves show $\tilde{n}_1(x, \tau)$ at time intervals of 0.2 up to $\tau = 2$.

both comminution and collection is the emergence of stationary solutions to the population balance equation. Here the effects of breakup are balanced by those of particle coalescence. Stationary solutions are readily obtained by the numerical method and are shown to be stable against changes in the initial function. The effects of particle growth can prevent stationary solutions from developing, however. The spline–Galerkin method should provide a useful tool with which to investigate numerical solutions of the population balance equation that arise in physical situations, for example, in gas–liquid and liquid–liquid dispersions.

REFERENCES

1. L. G. Austin, R. R. Kimpel, and P. T. Luckie, *Process Engineering of Size Reduction: Ball Milling* (Society of Mining Engineers of the American Institute of Mining, Metalurgical, and Petroleum Engineers, New York, 1984.
2. M. Barigou and M. Greaves, *Chem. Eng. Sci.* **47,** 2009 (1992).
3. P. S. Brown Jr., *J. Comput. Phys.* **58,** 417 (1985).
4. M. G. Cox, *J. Inst. Math. Appl.* **10,** 134 (1972).
5. C. deBoor, *J. Approx. Theory* **6,** 50 (1972).
6. C. de Boor, *A Practical Guide to Splines* (Springer-Verlag, New York/Heidelberg/Berlin, 1978).
7. L. D. Erasmus, D. Eyre, and R. C. Everson, *Comput. Chem. Eng.* **18,** 775 (1994).
8. D. Eyre, C. J. Wright, and G. Reuter, *J. Comput. Phys.* **78,** 288 (1988).
9. F. Gelbard and J. H. Seinfeld, *J. Comput. Phys.* **28,** 357 (1978).
10. J. W. Hilgers, R. J. Spahn, and T. H. Courtney, *Math. Modelling* **6,** 463 (1985).
11. P. C. Kapur, *Chem. Eng. Sci.* **27,** 425 (1972).
12. R. P. King, *South African Inst. Mining Metallurgy* **73,** 127 (1972).
13. T. W. Peterson, *Aerosol Sci. Technol.* **5,** 93 (1986).
14. M. J. Prince and H. W. Blanch, *AIChE J.* **36,** 1485 (1990).
15. D. Ramkrishna, *Rev. Chem. Eng.* **3,** 49 (1985).
16. G. W. Reuter, C. J. Wright, and D. Eyre, *J. Atmos. Sci.* **46,** 1407 (1989).
17. W. T. Scott, *J. Atmos. Sci.* **25,** 54 (1968).
18. T. Tobin, R. Muralidhar, H. Wright, and D. Ramkrishna, *Chem. Eng. Sci.* **45,** 3491 (1990).